International Journal of Electrical, Electronic and Communication Sciences
ISSN: 2517-9438
Vol:8, No:8, 2014

Prediction of the Performance of a Bar-Type Piezoelectric Vibration Actuator Depending on the Frequency Using an Equivalent Circuit Analysis

J. H. Kim, J. H. Kwon, J. S. Park, K. J. Lim

***Abstract*—**This paper has been investigated a technique that predicts the performance of a bar-type unimorph piezoelectric vibration actuator depending on the frequency. This paper has been proposed an equivalent circuit that can be easily analyzed for the bar-type unimorph piezoelectric vibration actuator. In the dynamic analysis, rigidity and resonance frequency, which are important mechanical elements, were derived using the basic beam theory. In the equivalent circuit analysis, the displacement and bandwidth of the piezoelectric vibration actuator depending on the frequency were predicted. Also, for the reliability of the derived equations, the predicted performance depending on the shape change was compared with the result of a finite element analysis program.

***Keywords*—**Actuator, performance, piezoelectric, unimorph.

I. Introduction

A piezoelectric transducer is a device that can convert electric energy to mechanical energy or vice versa. Representative examples include a piezoelectric actuator that converts electric energy to mechanical energy and a piezoelectric sensor that converts mechanical energy to electric energy. A piezoelectric actuator, which is also called a piezoelectric bender, produces vibration based on the deformation of a piezoelectric element to which voltage has been applied, or it is converted to other types of mechanical energy. A piezoelectric actuator is classified into unimorph, bimorph, and multilayer depending on the number of the layers of piezoelectric elements, and is classified into cantilever type, both ends supporting type, and center supporting type depending on the form of a support [1]-[5].

For achieving optimal design to be used in a specific device, it is important to derive performance, and thus, a lot of previous studies have been conducted. However, discussions have been mostly focused on the bender type for energy harvesting, the audio equipment such as a speaker and a buzzer, and the devices for transmitting mechanical forces such as a motor; and there are few studies on the design of haptic devices using a piezoelectric element. To control the noise of a specific device, Wang and Cross [5] studied a cantilever-type actuator using a piezoelectric element. They derived structural equations for all the shapes with unimorph, bimorph, and triple-layer benders by applying the balance equation, beam theory, and geometric compatibility condition, using the Wang and Cross method. Wood et al. [6] studied the design of a piezoelectric actuator for high energy density, and suggested an actuator design standard with the best performance based on the laminate plate theory, for a cantilever-type millimeter-scale bimorph actuator. The above-mentioned studies did not include a case in which the lengths of a metal plate and a piezoelectric element are different. Park et al. [7] supplemented this problem, and derived structural equations for all cantilever types based on the balance equation, beam theory, and geometric compatibility condition. Kohei Motoo et al. [8] studied cantilever-type and both ends supporting-type actuators based on dynamic analysis, and predicted the force and displacement performance of the actuators. However, the above-mentioned studies were mostly limited to the cantilever type, or considered a case in which the lengths of a metal plate and a piezoelectric element are identical even though the both ends supporting type was examined. In addition, they predicted the performance of an actuator only at a resonance frequency or at a single frequency.

This study examines a haptic actuator with various haptic effects, and an actuator with the performance of a wide bandwidth should be investigated. A haptic actuator for transmitting various haptic effects should have a fast response time, independently control the frequency and magnitude of vibration, and secure the frequency band of 0~200 Hz. A piezoelectric actuator can produce large force at a fast response time and a small size, and have a relatively wide operating frequency band, compared to the existing vibration motor that is used in mobile devices. Thus, it can implement various haptic effects, and is appropriate for small devices. Therefore, through dynamic analysis and equivalent circuit analysis, this paper aims to investigate a technique that predicts the performance of a bar-type unimorph piezoelectric vibration actuator, which can be applied to mobile devices, depending on the frequency. In the dynamic analysis, rigidity and resonance frequency, which are important mechanical elements, were derived using the basic beam theory. In the equivalent circuit analysis, the displacement and bandwidth of the piezoelectric vibration actuator depending on the frequency were predicted. Also, for the reliability of the derived equations, the predicted performance depending on the shape change was compared with the result of a finite element analysis program.

K.J.Lim is with the Dept. of Electrical and Electronic Engineering, Chungbuk National University, Korea (e-mail: kjlimg@gmail.com).

II. Dynamic Analysis and Equivalent Circuit Analysis Method

Fig. 1 shows the physical structure and components of the piezoelectric vibration actuator. The steel plate is fixed at both ends, and a polarized piezoelectric element is attached to the bottom of the steel plate in the thickness direction. The center of the steel plate is combined with high-density tungsten in order to appropriately adjust the resonance frequency of the actuator. The composite beam, where the steel plate and the piezoelectric element have been combined, experiences flexural deformation in the y-axis direction depending on the direction of the electric field applied to the piezoelectric element.

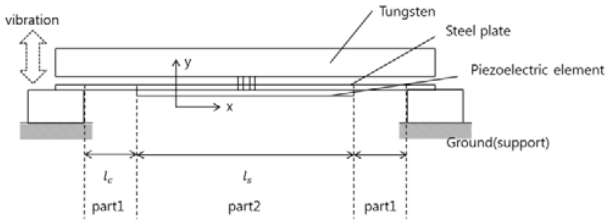

Fig. 1 Simple model for the sectional view of the actuator

A. Dynamic Analysis

In the model shown in Fig. 1, both ends of the beam are fixed at the supports on both sides. For the flexural deformation of the piezoelectric element where an electric field has been applied, the maximum bending occurs at the center of the beam. In this study, rigidity was obtained through dynamic analysis by dividing it into Part 1, which is a beam consisting of only the metal, and Part 2, which is a composite beam consisting of the combined metal and piezoelectric element. For Part 1, it has a cantilever shape where one side of the steel plate is fixed and the other side is free; the force applied to the end of the cantilever acts in the direction perpendicular to the plane of the steel plate; and the rigidity, $k_c = 3Y_m I_m/(l_c)^3$, if it is linear [9] where Y_m is the Young's modulus of the metal, I_m is the moment of inertia of Part 1, and l_c is the length of the cantilever. The moment of inertia, I_m, is expressed as $bt^3/12$.b and t referto the width and thickness of the steel plate in Part 1, respectively.

Part 2 has a composite beam shape where the metal plate and piezoelectric element are attached to each other. The rigidity of the composite beam, $k_s = 48Y_m I_t/(l_s)^3$. $I_t$is the moment of inertia of the composite beam, and l_s is the length of the composite beam. The moment of inertia of the composite beam can be obtained using the section transformation method. In the section transformation method, the section of the composite beam is transformed into an equivalent section consisting of a single material. For the transformation, the modular ratio, β, is defined as the ratio of the Young`s modulus of the constituting materials. In this study, the length of the piezoelectric element section's width was transformed, and it was assumed to be a single material, as shown in Fig. 2. Therefore, for the moment of inertia of the transformed section, the moment of inertia for the neutral axis of the entire section can be expressed as (1) using the parallel axis theorem [10].

$$I_t = I_m + \beta I_p \tag{1}$$

whereI_m,$I_p$are the moment of inertia of the steel plate and the piezoelectric element, respectively, and β=Y_m/Y_p.

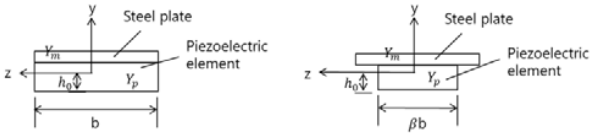

Fig. 2 Transformed cross section of the composite beam

The composite rigidity of the actuator shown in Fig. 1 can be regarded as two springs where the rigidity of Part 1 and Part 2 are connected in series. Thus, it can be expressed as (2).

$$k_t = (\frac{1}{k_c} + \frac{1}{k_s} + \frac{1}{k_c})^{-1} \tag{2}$$

B. Equivalent Circuit Analysis

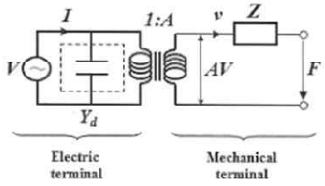

Fig. 3 Equivalent circuit of electro-mechanical energy transmission system

Using an electroacoustic theory, a piezoelectric vibrator can be expressed as an equivalent circuit including an electric terminal and a mechanical terminal, as shown in Fig. 3. In this circuit, the force, F, and the current, I, can be expressed as (3) [11].

$$\mathrm{F} = \mathrm{AV} - \mathrm{Z}\nu\,, \mathrm{I} = Y_d V + A\nu \tag{3}$$

where F is the force, A is the force factor, V is the voltage, Z is the mechanical impedance of the piezoelectric element, and ν is the velocity. If the internal mechanical impedance, Z, and the impedance reduction due to the velocity, ν, are excluded, the force factor, A, can be expressed as the force, F, per applied unit voltage. In this regard, as it is a rectangular parallel piped-shaped plate polarized in the thickness direction, the force factor, A, can be expressed as (4) using the width of the piezoelectric element, b_p, piezoelectric constant, d31, and Young's modulus,Y_{11}.

$$\mathrm{A} = b_p d_{31} Y_{11} \tag{4}$$

In addition, mass, rigidity, and damping, which are mechanical parameters, can be converted to electric elements along with the force factor. As shown in Fig. 4, mass corresponds to the inductance of the electric circuit, L, rigidity

corresponds to the capacitance, C, and internal damping corresponds to the resistance, R. Thus, they can be expressed as (5). R is damping, which is a property that suppresses the vibration of an object, and represents the structural vibration damping, $R = 2k_t\beta/(2\pi f_0)$due to the internal damping of the material. $k_t$is the total rigidity, f_0 is the resonance frequency, and β is the constant.

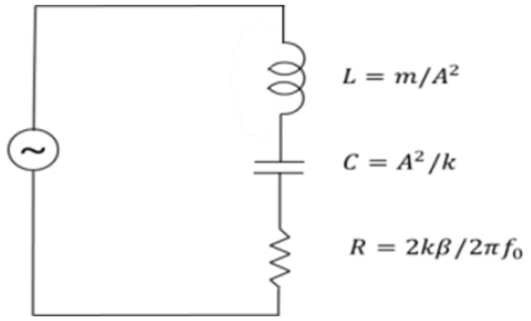

Fig. 4 Equivalent circuit for the model in Fig. 1

$$\frac{m}{A^2}\frac{d^2q}{dt^2} + \frac{2k_t\beta}{2\pi f_0}\frac{dq}{dt} + \frac{k_t}{A^2}q = \frac{f(x)}{A} \quad (4)$$

III. Numerical Result and Discussion

In this section, the predicted performance of a piezoelectric vibration actuator depending on the thickness and width of the piezoelectric element, the Young's modulus of the steel plate, and the mass of tungsten was examined using the analysis method suggested in this study. For the piezoelectric vibration actuator having the standard specification summarized in Table I, the rigidity of part 1, k_c, and total rigidity, k_t, were corrected by the multiplication of the correction factors, α,γ, respectively, through the comparison with the results of a finite element analysis simulation, and the constant, β, of the vibration damping, R, was also calculated based on the results of a finite element analysis simulation (α=3.375,γ=1.6,β=0.015). Thus, the displacement and vibration acceleration for a frequency can be expressed as follows, based on (4).

$$\mathrm{d} = \frac{V}{\sqrt{\left(\frac{2k_t\beta}{\omega}\right)^2 + \left(\omega\frac{m}{A^2} - \frac{\gamma k_t}{\omega A^2}\right)^2}},\ \mathrm{a} = \frac{\omega^2 \times d}{9.8 * m} \quad (5)$$

where the preset voltage is 150 V_{pp}, and m is the sum of the mass of tungsten and the mass of the piezoelectric element and the steel plate. The range of the input frequency was set to 100~300 Hz, which is an optimal frequency band considering the vibration sensitivity of a human. The dimensions and material properties of the piezoelectric vibration actuator summarized in Table I was used as the basic specification, and the performance was predicted based on an equivalent circuit analysis by changing the above-mentioned four parameters.

Figs. 5-8 show the prediction results of the vibration acceleration for a frequency depending on the change in the parameter, based on the equivalent circuit analysis of the piezoelectric vibration actuator.

Fig. 5 shows the comparison between the prediction result of the equivalent circuit analysis and the result of the FEM simulation when the thickness of the piezoelectric element was changed from the standard specification presented in Table I. The dotted line represents the result of the FEM simulation, and the solid line represents the prediction result. Fig. 5 shows the comparison between the prediction result and the FEM simulation result for the maximum vibration acceleration and the resonance frequency depending on the thickness of the piezoelectric element. As the thickness of the piezoelectric element decreased, the displacement increased due to the decrease in the vibration damping (R). However, the resonance frequency decreased, and thus the maximum vibration acceleration decreased. In addition, the bandwidth for each condition was calculated as R/L. The decrease in the value of the vibration damping (R) was relatively larger than that of the inductance (L). Thus, the bandwidth showed a decreasing trend as the thickness of the piezoelectric element decreased. As shown in Fig. 5, the highest vibration acceleration and the widest bandwidth could be obtained when the thickness of the piezoelectric element was 0.3 mm.

TABLE I
Material Properties and Dimensions of the Piezoelectric Actuator

	Piezoelectric element	Steel plate	Tungsten mass
Length (mm)	30	42	38
Width (mm)	2	2	2
Thickness (mm)	0.3	0.2	1.5
Young`s modulus ($10^9 N/m^2$)	65	210	N/A
Density ρ (kg/m^3)	7500	7800	17470
Piezoelectric strain constant d_{31} (10^{-12}m/V)	-123	N/A	N/A
Weight (g)	0.135	0.131	1.99

Fig. 6 shows the prediction result and the simulation result for the performance variation when the mass of tungsten in the piezoelectric vibration actuator was changed. When the mass of tungsten was increased from the standard specification to 2.323 g and 2.655 g, the changes in the displacement of the piezoelectric vibration actuator were insignificant in both the prediction result and the simulation result. However, the maximum vibration acceleration showed a decreasing trend due to the decrease in the resonance frequency. The bandwidth decreased depending on the increase in the inductance (L) because the change in the value of the vibration damping (R) was small. As shown in Fig. 6, the maximum vibration acceleration was the lowest when the mass of tungsten was 1.99 g. However, the tungsten mass of 1.99 g with the widest bandwidth needs to be selected, provided that enough stimuli can be transmitted when used in a specific device.

Fig. 7 shows the prediction result and the simulation result for the performance variation when the Young's modulus of the steel plate was changed. The Young's modulus of the steel plate of the standard specification was changed into 170 GPa and 210 GPa, and the result of the bandwidth was examined. In the prediction result, as the Young's modulus of the steel plate increased, the displacement decreased due to the increase in the rigidity (k). However, due to the increase in the resonance

frequency, the maximum vibration acceleration and the bandwidth showed an increasing trend as the Young's modulus increased. On the other hand, in the simulation result of the maximum vibration acceleration, the range of variation depending on the Young's modulus was larger than that in the prediction result. In the simulation result, as the Young's modulus of the steel plate decreased, the displacement of the piezoelectric vibration actuator also decreased, unlike the predicted displacement. The condition for deriving the rigidity of Part 1 was the case in which force is applied to the end of the cantilever in the direction perpendicular to the plane of the beam. However, for the model shown in Fig. 1, the force generated at the end of the cantilever in Part 1 by the bending of the piezoelectric element to which voltage has been applied is not perpendicular to the plane of the beam. To correct this, a correction factor was inserted. However, it is thought that the prediction result depending on the change in the specific variable would include an error to a certain extent as shown in the result in Fig. 7. The highest vibration acceleration and the widest bandwidth could be obtained when the Young's modulus of the steel plate was 250 Gpa, as shown in Fig. 7.

Fig. 8 shows the prediction result and the simulation result for the performance variation when the width of the piezoelectric element was changed. In this regard, the width of the steel plate was also changed identically. As the width of the piezoelectric element increased, the force factor increased. However, the displacement showed a decreasing trend because the range of increase in the rigidity was large. As shown in Fig. 8, in the simulation result of the maximum vibration acceleration, the range of variation depending on the change in the width of the piezoelectric element was larger than that in the prediction result. This is thought to be because if the width of the piezoelectric element decreases on a simulation, the displacement of the actuator also decreases; and is also thought to be due to the effect of Part 1 mentioned earlier. As shown in Fig. 8, the force factor was the highest and the bandwidth had the maximum value when the width of the piezoelectric element was 2.5 mm.

To summarize the prediction results shown in Figs. 5-8, for the piezoelectric vibration actuator shown in Fig. 1, the vibration acceleration and the bandwidth increased as the thickness of the piezoelectric element was changed from 0.15 mm to 0.3 mm; and the vibration acceleration decreased but the bandwidth increased as the mass of tungsten was changed from 2.655 g to 1.99 g. When the Young's modulus of the steel plate and the width of the piezoelectric element were changed, the vibration acceleration and the bandwidth increased as the Young's modulus increased and as the width of the piezoelectric element increased. In particular, when the width of the piezoelectric element was 2.5 mm, the bandwidth was wider than any other bandwidths obtained when other parameters were changed.

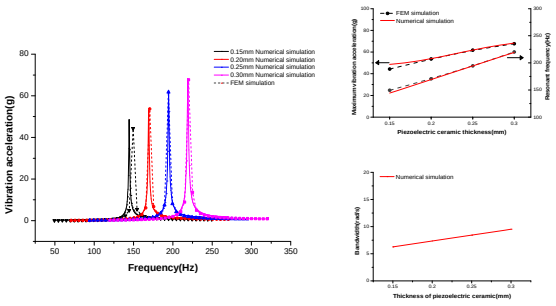

Fig. 5 Prediction results by changing piezoelectric element thickness

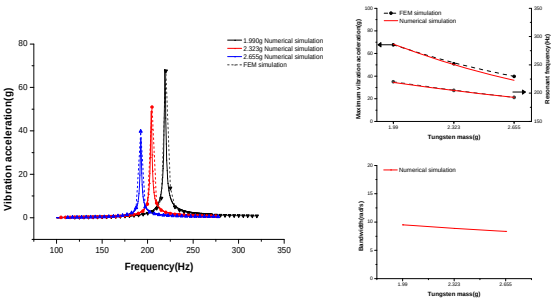

Fig. 6 Prediction results by changing tungsten mass

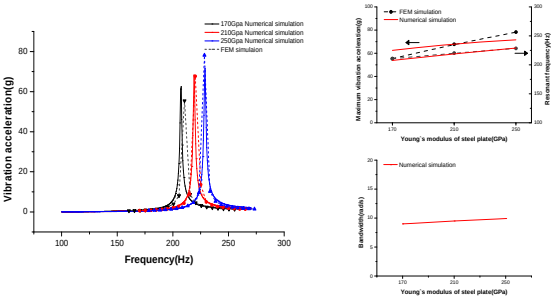

Fig. 7 Prediction results by changing Young`s modulus of steel plate

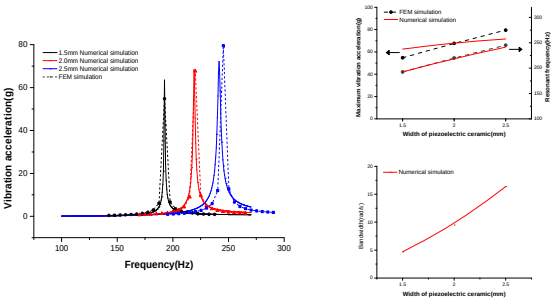

Fig. 8 Prediction results by changing width of steel plate

IV. Conclusion

This paper have been investigated a technique that predicts the performance of a bar-type unimorph piezoelectric vibration actuator depending on the frequency. This paper has been proposed an equivalent circuit that can be easily analyzed for

the model in Fig. 1. Compared with the result of a finite element analysis program, the results that predicted based on an equivalent circuit analysis by changing the four parameters have shown a similar tendency. In future studies, the technique can be improved by comparing the experiment results and will consider a transient response of piezoelectric vibration actuator.

ACKNOWLEDGMENT

This work was supported by the research grant of Chungbuk National University in 2013

REFERENCES

[1] F. Zhang, A. Li, X.Li, Min Chen, and Y. Ren, Proceedings of the 2011 IEEE International Conference on Robotics and Biomimetics(Phuket, Thailand, 2011) p.2762.
[2] S.T.Todd and H.Xie, j.Microelectromechanical System. 17, 213(2008)
[3] H.Chen, D.Jin, and Z. Meng, Proceedings of the 6th International Conference on Properties and Applications of Dielectric Materials (Xi`an Jiaotong University, Xi`an, China, 2000) p.983.
[4] W.P. Robbins and D.E. Glumac, Trans. Ultrasonic. Ferroelectr. Freq. Control. 45, 1151 (1998).
[5] Q.M.Wang and L.E.Cross, Trans. Ultrasonic. Ferroelectr. Freq. Control. 46, 1343 (1999).
[6] R.J.Wood, E.Steltz, and R.S.Fearing, j.Sens. Actuator A, 119,476(2005)
[7] J.K.Park and W.K. Moon, j.Sens. Actuator A, 117, 159(2005).
[8] K.Motoo, N.Toda, T.Fukuda, F.Arai, K.Kikuta,S.Hirano, and T.Matsuno, International Symposium on Micro-Nano Mechatronics and Human Science (Nagoya, Japan, 2006).
[9] B.balachandran and E.B.Magrab, Vibrations (Thomson, Asia, 2005) p.33.
[10] J.M.Gere, Mechanics of Materials (Thomson, Asia,2001) p.427.
[11] T.Sashida, An Introduction to Ultrasonic Motors (Oxford, New York, 1993) p.55.

J. H Kim (B.S'13) received B.S degree in electrical engineering from Chungbuk National University, Korea. Currently he is a student in the Master's course of the Department of Electrical Engineering, Chungbuk National University, Korea

J. H Kwon (M.S'13) received the B.S. and M.S. degree in 2011 and 2013 in electrical engineering from Chungbuk National University, Korea. Currently he is a student in the Ph.D. course of the Department of Electrical Engineering, Chung-buk National University, Korea.

J. S. Park (B.S'14) received the B.S degree in 2014 in electrical engineering from Chungbuk National University, Korea. Currently he is a student in the Master's course of the Department of Electrical Engineering, Chungbuk National University, Korea.

K. J. Lim received B.S. M.S. and Ph.D. degrees from Han-Yang University, Seoul, Republic of Korea, in 1973, 1979 and 1986. He is currently a full professor with dept. of electrical engineering at Chungbuk National University, Korea. His research interests include electrical materials, high voltage techniques, piezoelectric ceramics and so on.